

Fiber Architecture of Three-Dimensional Braided Composites

Soheil Mohajerjasbi*

Boeing Defense & Space Group, Philadelphia, Pennsylvania 19142-0858

The fiber architecture of a three-dimensional braided composite is demonstrated. A preform produced by the (1×1) braiding process is considered, and section cuts of different areas of the composite are presented. The type A and type B interior cells, which were identified previously, are used to construct these cross sections. The different yarn orientations in the interior, boundaries, and corners of the composite are also shown. These differences in fiber architecture result in different stiffness properties and are expected to affect the mechanical properties of the composite. The relative influence of different fiber architectures in the boundaries and corners is evaluated by two simple methods. This evaluation suggests that, for the range of three-dimensional braided preforms currently produced, the effect of boundaries and corners may not be negligible. It is also shown that the fiber architecture in the corners of the preform may vary depending on the number and arrangement of yarn carriers on the braiding machine. Finally, photographs of different cross sections of a three-dimensional braided specimen are provided for comparison and verification of the fiber architecture.

Introduction

THE fiber architecture and mechanical properties of composites fabricated by the three-dimensional braiding process are of interest because of their potential for reducing manufacturing cost. This cost reduction is envisioned in automation, use of fiber and matrix in their lowest cost form, and the capability of this process to produce near-net-shape composite parts. In addition, compared with conventional laminated composites, three-dimensional braided composites have superior delamination resistance and energy absorption capability. A correct understanding and representation of the fiber architecture are essential for developing analytical models for prediction of stiffness and strength of these composites and for developing design guidelines.

The fiber architecture of the three-dimensional braided composite is different from, and more intricate than, conventional laminated composites due to the three-dimensionally integrated nature of the preform. Traditionally, the three-dimensional braided composite has been idealized as a "unit cell" in the form of a cuboid with lines, which represent the yarns, connecting diagonally between the opposite corners. However, more recent research¹ has shown that the three-dimensional braided composite is composed of different fiber architectures in the interior, boundaries, and the corners. The description and presentation of the fiber architecture of three-dimensional braided composites present a few challenges, however. First, the three-dimensional braided composite is the product of a fabrication process that needs to be understood to gain insight into the form of its product. In fact, the movements associated with the braiding machine will determine the fiber architecture of the composite, and any attempt to define the fiber architecture divorced from the operation of the braiding machine will not be very meaningful. Second, it is difficult to present the three-dimensional structure of the three-dimensional braided composite in a two-dimensional medium. Third, the fiber architecture of the composite needs to be presented in a manner that would facilitate its experimental verification. To make the fiber architecture easier to understand, and perhaps to be able to verify it experimentally, a presentation methodology is adopted here that uses the microstructure identified previously as building blocks to reveal the fiber architecture on a macro scale.

In this paper, the fiber architecture of the interior of the three-dimensional braided composite, which was previously identified on the basis of the movements of the braiding machine as type A and

type B interior cells, is briefly reviewed. Then the fiber architecture of the preform is shown in somewhat more detail by providing section cuts of different areas of the composite. The type A and type B interior cells are used to construct these cross sections. The differences of orientation of the yarns in the interior, boundaries, and corners are pointed out on these cross-sectional views. It is also shown that the fiber architecture in the corners of the preform may vary depending on the number and arrangement of yarn carriers on the braiding machine. Finally, photographs of different cross sections of a braided specimen are provided for comparison and verification.

Fiber Architecture

The term fiber architecture refers to the yarn structure in the preform that, in the context of this paper, is the product of a textile fabrication process referred to as three-dimensional Cartesian braiding. A schematic of a braiding machine is shown in Fig. 1. In this process yarns (fiber bundles) are loaded on yarn carriers, which are then arranged in rows and columns on the machine bed (X - Y plane) in a form similar to the shape of the preform to be produced. The ends of the yarns are tied to a movable plate above the braiding machine. The yarn carriers on the machine bed are moved in a prescribed manner, as a result of which the preform is produced above the machine. For the purpose of demonstration, a (1×1) braiding process is considered here. In this process, the yarn carriers are moved by one carrier spacing in the x and then the y direction in each machine step. This braiding process is also referred to as a four-step process, as an identical carrier configuration is obtained after each four machine steps. The operation of the three-dimensional Cartesian braiding machine is explained in more detail in Ref. 2.

Once the preform is fabricated, it is consolidated with a matrix material to obtain a braided composite. The yarn structure of the braided composite produced in four machine steps is referred to as a "repeat unit." The height h of the repeat unit is known as a pitch. Any subsequent machine operation is a repeat of these four steps and will produce a yarn structure that is identical to the one produced in these four steps. A schematic of a square-shaped braided composite that represents the product of a (1×1) braiding operation with an array of 10×10 yarn carriers on the machine bed, designated as $[10 \times 10]$, is shown in Fig. 2. Three repeat units are shown in this schematic.

On the basis of an examination of the operation of the braiding machine and movements of the yarn carriers, it was shown in Ref. 2 that a simple way of showing the yarn structure in the interior of the composite is by representing it as a repetition of type A and type B cells. These two cell types are shown with different shadings in Fig. 2. In the interior of the composite, these two cell types alternate along 45 and 135 deg measured from the x axis. The top view of this preform is again shown in Fig. 3a, where the interior is represented in terms of type A and type B cells. Also shown in Fig. 3b is a

Received March 4, 1997; presented as Paper 97-1404 at the AIAA/ASME/ASCE/AHS/ASC 38th Structures, Structural Dynamics, and Materials Conference, Kissimmee, FL, April 7-10, 1997; revision received Sept. 25, 1997; accepted for publication Dec. 31, 1997. Copyright © 1998 by Soheil Mohajerjasbi. Published by the American Institute of Aeronautics and Astronautics, Inc., with permission.

*Staff Engineer, Helicopters Division, P.O. Box 16858, MS P 38-13, Member AIAA.

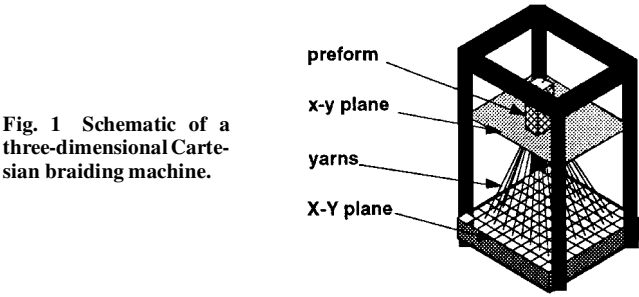


Fig. 1 Schematic of a three-dimensional Cartesian braiding machine.

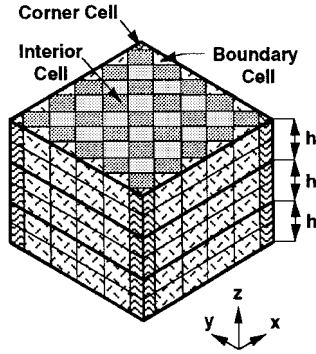


Fig. 2 Schematic of a three-dimensional braided preform using [10 x 10] yarn carriers.

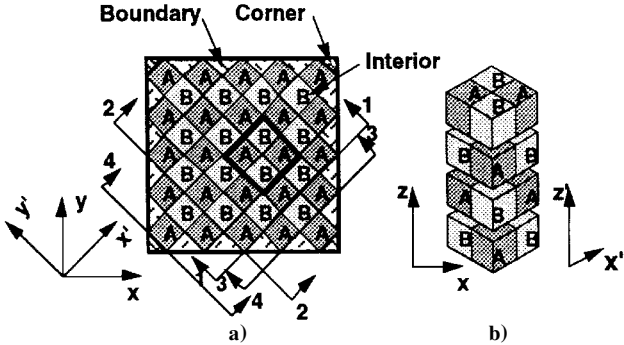


Fig. 3 Top view and cutaway view of the interior of three-dimensional braided composite.

cutaway view of the preform to show the arrangement of the two cell types along the length of the preform. It can be seen that type A and type B cells alternate along the axis of the braided preform (z axis) as well. Also, by examination of the operation of the braiding machine it was noted that each yarn from the interior enters the boundary and over a distance of one pitch h changes direction and enters the interior again. Similarly, each yarn that enters the corner from the interior changes direction and over a distance of $3h/2$ enters the interior again. As a result, the fiber architectures at the boundaries and corners were found to be different from the interior. These different yarn structures in the boundaries and corners of the preform are represented in Figs. 2 and 3a by different shadings.

As shown in Fig. 4, the type A and type B cells consist of cuboids that represent the matrix material, encapsulating the yarn pieces that are represented by their centerlines as straight lines. The angle between the centerline of the yarns in the interior and the axis of the braided preform (z axis) is referred to as the interior braiding angle γ . Also shown in Fig. 4 are intersections of the type A and type B cells with three planes parallel to the top and the sides of the cuboids. These cross sections are identified with the same numbering system shown on the corners of the cells; e.g., the cross section identified with corners 1, 2, 6, and 5 is parallel to the side of the cuboid having 1, 2, 6, and 5 as corners. The cross sections identified with corners 5, 6, 7, and 8 are parallel to the x - y plane, whereas cross sections identified with corners 1, 2, 6, and 5 make an angle of 135 deg with the x axis, and cross sections identified with corners 2, 3, 7, and 6 make an angle of 45 deg with the x axis. The cross sections of the yarns, which are assumed to be circular cylinders, are also shown on these cutting planes. This is only an idealization, and depending on the influence of the neighboring yarns inside the preform, the cross section of the actual yarn may vary along its length.

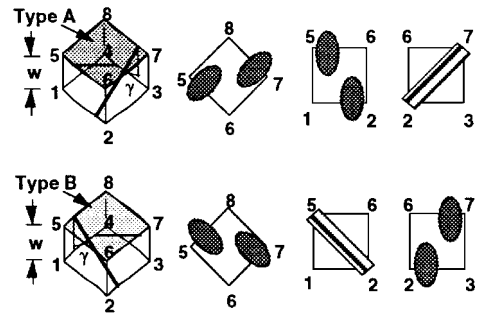


Fig. 4 Type A and type B interior cells and intersections with x - y , 45-deg, and 135-deg planes.

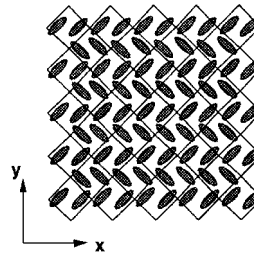


Fig. 5 Cross section of three-dimensional braided composite parallel to x - y plane.

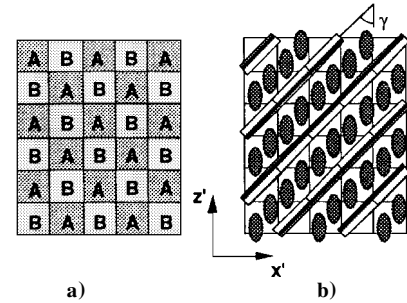


Fig. 6 Cross section of three-dimensional braided composite taken at 45 deg to x axis.

The preceding information regarding the fiber architecture was derived as a result of observing the movements of the fiber carriers on the braiding machine.² In what follows, this information is used to construct views of cross sections of the composite parallel to the x - y plane and parallel to planes making 45 and 135 deg with the x axis, respectively. This is done with the aid of the cross sections of the two cell types shown in Fig. 4. Also, for the purpose of verifying the constructed cross sections, a braided specimen is cut along similar planes, and photographs of those cross section are provided for comparison later in this paper.

A cross section of the braided composite parallel to the x - y plane is shown in Fig. 5. Figure 3a and cross sections of type A and type B cells identified with corners 5, 6, 7, and 8 in Fig. 4 are used to construct this cross section.

Note that only the cross section of the yarns in the interior of the preform is shown. Also, because the type A and type B cells alternate along the z axis (Fig. 3b), a cross section parallel to the x - y plane and shifted by $h/2$ below or above this section would be slightly different, as explained next. From Fig. 4 it can be seen that the difference between the intersection of the x - y plane and type A and type B cells (cross sections identified with corners 5, 6, 7, and 8) is the inclination of the ellipses, which represent the intersection of the circular yarns with the x - y plane.

Now to show a cross section of the interior of the composite consider section 1-1 taken at 45 deg from the x axis, shown in Fig. 3a. The arrangement of the type A and type B cells at this section is shown in Fig. 6a, and using the cross sections identified with corners 2, 3, 7, and 6 in Fig. 4, the cross section of the composite at section 1-1 is shown in Fig. 6b.

Similarly, the cross section at section 2-2 in Fig. 3a, which is at 135 deg from the x axis, may be constructed as shown in Fig. 7b. The arrangement of the type A and type B cells at section 2-2, which is shown in Fig. 7a, and cross sections identified with corners 1, 2, 6, and 5 in Fig. 4 are used to construct this cross section.

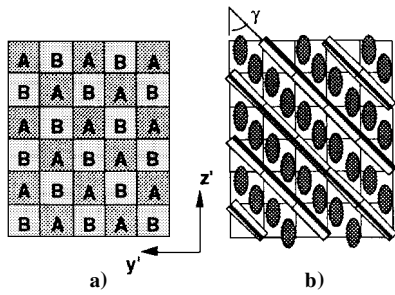


Fig. 7 Cross section of three-dimensional braided composite taken at 135 deg to x axis.

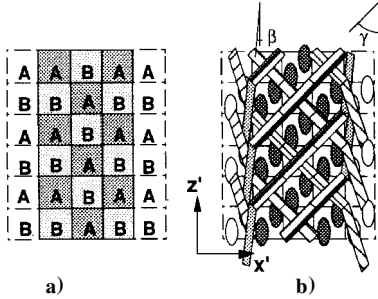


Fig. 8 Cross section of the boundaries of three-dimensional braided composite.

Note that, if section 1-1 was taken one-half of a cell width away from its present location shown in Fig. 3a, thereby cutting the type A and type B cells in the middle, the second yarns in each cell would become visible and the cross section at 1-1 would have been identical to that shown in Fig. 7b. Similarly, if section 2-2 was taken one-half of the cell width away from its present location shown in Fig. 3a, the cross section at 2-2 would have been identical to that shown in Fig. 6b.

Figures 6b and 7b show that the yarns in the interior of the composite are inclined at an angle γ with respect to the z axis and traverse the width of the preform without changing direction in the interior.

To show a cross section of the boundary of the composite, section 3-3 in Fig. 3a is considered. It is seen from Fig. 3a that, at section 3-3, three interior cells are immediately in front of the section line and two other interior cells, one on each side, are farther away. The arrangement of the interior cells at this section is shown in Fig. 8a. The interior cells on either side, which are farther away from the section line, are shown with dash lines and without any shading. The spaces on either side between the outer dash lines and immediate solid lines represent the boundary cells. Here, one needs to show both yarn pieces inside the interior cells, and it may be helpful to visualize the matrix material as transparent so that when cross sections of the cells in Fig. 4 are viewed, the second yarn piece is partially visible behind the yarn piece in the foreground. The yarns in the interior and the fiber architecture in the boundary cells are shown in Fig. 8b. It can be seen that each yarn from the interior enters the boundary and over a distance of one pitch h changes direction and enters the interior again. It is noted in Fig. 8b that the angle between the yarns in the boundary and the z axis, β , is smaller than the interior braiding angle γ . This implies that in the z direction (i.e., along the length of the preform) the boundaries have a higher stiffness than the interior.

The interior braiding angle γ cannot be measured directly as it represents the yarn orientation inside the preform. However, it can be calculated from three parameters, u , v , and w , which may be measured from the surfaces of the braided composite. Figure 9 shows a view of the surface of the preform and definitions for the parameters u and w . The parameter v is measured similar to u but from the other surface (parallel to the y axis) of the braided composite. In Fig. 9 the surface yarns are shown in an open position for demonstration purposes, whereas the yarns on the surfaces of the braided parts are tight, a conditioned referred to as jamming.

The relationship between u , v , w , the surface angle θ , and the interior braiding angle γ may be expressed as follows:

$$\tan \theta = 2u/2h = u/2w \quad (1)$$

$$\tan \gamma = 2\sqrt{1 + (u^2/v^2)} \tan \theta \quad (2)$$

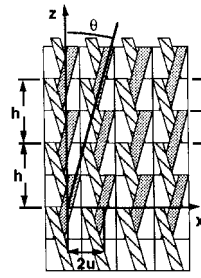


Fig. 9 View of the surface of three-dimensional braided composite.

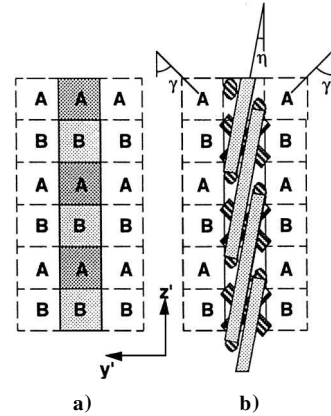


Fig. 10 Cross section of the corner of three-dimensional braided composite.

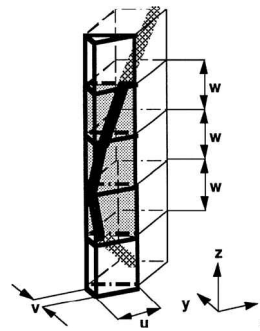


Fig. 11 Path of one yarn in the corner of three-dimensional braided composite.

To show a cross section of the corner of the composite, section 4-4 in Fig. 3a is considered. It is seen from Fig. 3a that, at section 4-4, one interior cell is immediately in front of the section line and two other interior cells, one on each side, are farther away. The space on either side between the outer interior cell and the interior cell immediately in front of the section line represents the boundary cell. The arrangement of the interior cells at this section is shown in Fig. 10a. Again, the interior cells on either side are shown with dash lines. The view of the corner of the composite is shown in Fig. 10b. The cross sections identified with corners 1, 2, 6, and 5 in Fig. 4 and the cross section in Fig. 10a are used to construct this view. Both yarn pieces inside the interior cells forward of the section line are shown on the cross section, as well as the interior braiding angle γ . It can be seen that each yarn from the interior enters the corner and over a distance of $3h/2$ changes direction and enters the interior again. It is noted from Fig. 10b that the angle between the yarns in the corner and the z axis, η , is smaller than the interior braiding angle γ .

From the geometry of the three-dimensional braided preform shown thus far, it can be seen that with respect to the z axis the angle of inclination of the yarn in the corner is smaller than that in the boundary, which in turn is smaller than the angle of inclination of the yarn in the interior. This implies that in the z direction the corners have higher stiffness than the boundaries, which in turn have higher stiffness than the interior.

Figure 11 shows a perspective view of the corner of the preform and demonstrates the path of one yarn as it enters the corner from the interior, changes direction, and re-enters the interior again.

Having shown that the fiber architectures in the interior, the boundaries, and the corners are all different, two questions remain. First, are these differences important enough to affect the

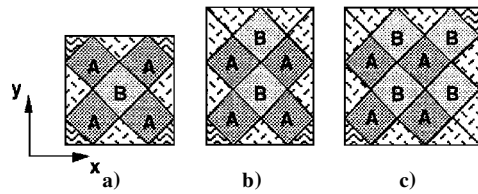


Fig. 12 Repeat unit for a) $[4 \times 4]$, b) $[4 \times 5]$, and c) $[5 \times 5]$ preforms.

mechanical properties of the composite, and second, will all three-dimensional braided composites have a repeat unit similar to that shown in Fig. 3a.

Recently, some authors, while acknowledging the differences in the fiber architecture stated earlier, have suggested (without any reasoning or justification) that the contributions of the surface and corners are expected to be small. Two ways to evaluate the relative importance of the boundaries and the corners are considered in the following. The first is based on the ratio of the number of the yarns in the interior to the total number of yarns in the preform. For an $[M \times N]$ preform (M and N being the number of yarn carriers on the machine bed along the X axis and Y axis, respectively), the number of yarns in the interior is $M \times N$, whereas the total number of yarns on the braiding machine is $(M \times N) + (M + N)$. The ratios of the number of interior yarns to the total number of yarns for a $[4 \times 4]$, $[6 \times 6]$, and $[10 \times 10]$ preform are 67, 75, and 83%, respectively. Another approximate way of evaluating the relative importance of the boundaries and corners is to consider the ratio of the volume of the interior cells to the total volume of the repeat unit. These ratios for a $[4 \times 4]$, $[6 \times 6]$, and $[10 \times 10]$ preform are 63, 72, and 82%, respectively. It is seen that as the number of the yarns increases, with an attendant increase in the size of the preform, these ratios grow closer to 100%. The fact that about 17% of a $[10 \times 10]$ braided composite is composed of boundary and corner cells, which as shown earlier have higher axial stiffness than the interior cells due to smaller yarn angles (Figs. 8b and 10b), suggests that at least for the size range of preforms currently produced the effect of boundaries and corners may not be small. Additionally, there is evidence of drastically reduced mechanical properties in specimens with cut edges compared with specimens with uncut edges.^{3,4}

As to the second question, observation of the movement of $[M \times N]$ yarn carriers on the machine bed suggests that the form of the repeat unit will be similar to that shown in Fig. 3a for a $[10 \times 10]$ preform as long as M and N are both even numbers. If either M or N or both are odd numbers, the form of the corners of the repeat unit would be different.

Figure 12 shows the repeat units of a $[4 \times 4]$, a $[4 \times 5]$, and a $[5 \times 5]$ preform. The interior is again identified with type A and type B cells. It can be seen from Fig. 12a that the $[4 \times 4]$ preform has four corner cells similar to the $[10 \times 10]$ preform shown in Figs. 2 and 3a, but for the $[4 \times 5]$ preform shown in Fig. 12b, the upper corner cells are missing and two boundary cells come together to form the upper corners of the preform. Also, in Fig. 12c it can be seen that for the $[5 \times 5]$ preform the corner cells in the lower right and upper left of the preform are missing and two boundary cells come together to form the corners of the preform in these locations. Again, these differences in fiber architecture of the corners depending on the number and arrangement of the yarn carriers on the machine bed are more reasons that, at least for the size range of preforms currently produced, the effect of boundaries and corners may not be ignored.

Verification of Fiber Architecture

For the purpose of verifying the constructed cross sections, a braided specimen is cut along similar planes, and photographs of these cross sections are provided for comparison. The preform for this specimen was braided at Drexel University using glass yarns and was consolidated with PR500 resin via Resin Transfer Molding (RTM) at Boeing. The fabrication of the preform was carried out on a semiautomatic braiding machine, which required a good deal of hand work. Even though the general appearance and the quality of the fabricated preform were judged to be very good, it was obvious that slight nonuniformities, attributable to the machine operator, were introduced during the fabrication of the preform. Some of these nonuniformities are evident in these photographs.

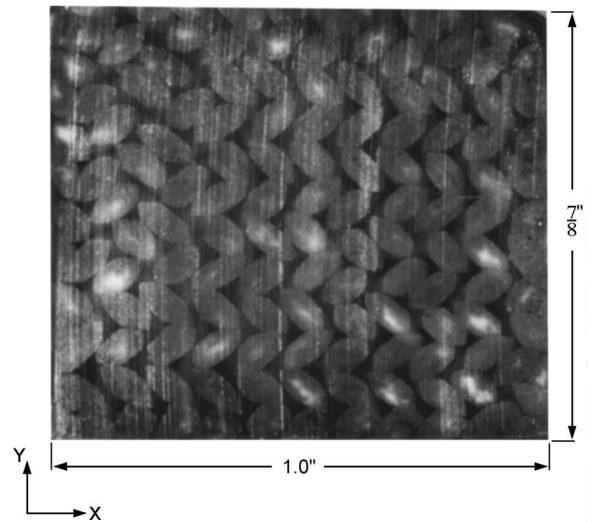


Fig. 13 Cross section of three-dimensional braided specimen parallel to x - y plane.

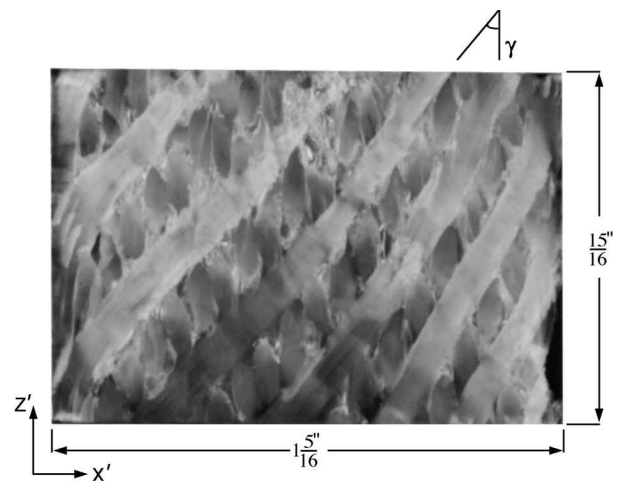


Fig. 14 Cross section of three-dimensional braided specimen at section 1-1.

For the following explanation it may be helpful to refer to the schematic of the preform and the coordinate system of the composite shown in Figs. 2 and 3a. A cross section of the specimen parallel to the x - y plane is shown in Fig. 13. Even though the pattern in the interior of this specimen resembles the cross-sectional view shown in Fig. 5, there are slight differences. The reason for these differences was explained earlier following the description of Fig. 5. Also, it can be seen in Fig. 13 that the pattern in the interior is different from the edges and the corners. This is due to different fiber architecture of the boundaries and corners, which was explained earlier.

Figure 14 shows a cross section of the interior of the braided specimen at section 1-1 in Fig. 3a. Again, the resemblance between Figs. 6b and 14 is noteworthy. The angle of inclination of interior yarns in this figure with respect to the z axis is what was earlier defined as the interior braiding angle γ . Also, Fig. 14 partially shows the yarns in the boundaries of the composite. It can be seen that the angles of inclination of yarns on the left and right sides of the photograph are different from those of the yarns in the interior.

Figure 15 shows a cross section of the braided specimen, similar to section 3-3 in Fig. 3a, to demonstrate the yarns in the boundaries. The changes in the angles of the yarns as they enter the boundaries are evident on both sides of this photograph. It is noted that only one of the two yarns in the boundaries is visible, as compared with Fig. 8b, where both yarns in the boundaries are shown.

A cross section of the corner of the specimen, similar to section 4-4 in Fig. 3a, is shown in Fig. 16. It can be seen that the paths of the yarns in the corner are similar to those shown in Figs. 10b and 11.

As was stated earlier, the different fiber architectures in the boundaries and corners are expected to affect the mechanical properties of the composite. A finite element based modeling approach, which

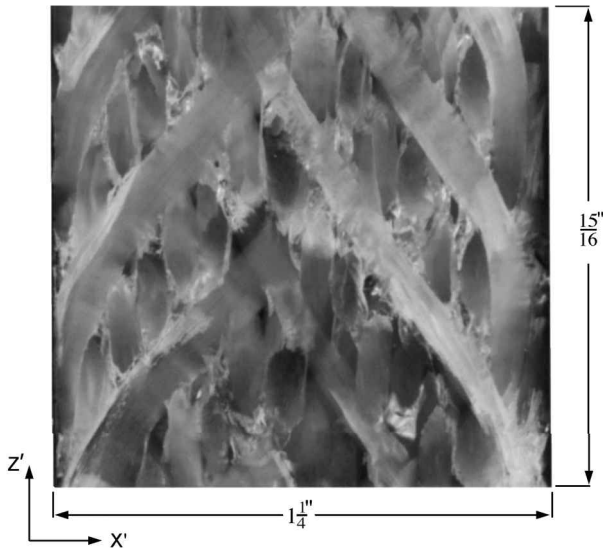


Fig. 15 Cross section of three-dimensional braided specimen at section 3-3.

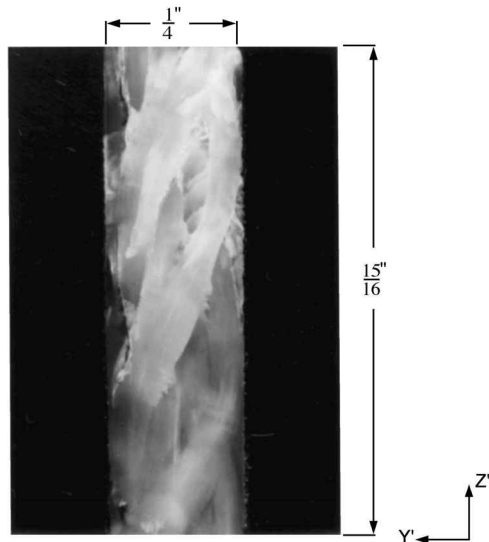


Fig. 16 Cross section of three-dimensional braided specimen at section 4-4.

accounts for the different fiber architectures in the interior, boundaries, and corners, was previously proposed,¹ and predictions for the elastic constants² and coefficients of thermal expansion⁵ were reported. The predictions of this modeling approach¹ indicate that for small braided preforms the boundary and corner regions could have a significant influence on the axial stiffness of the composite.

Summary and Conclusion

The fiber architectures of the interior, boundaries, and corners of a three-dimensional braided composite are demonstrated. Previously identified microstructure is used to construct different cross sections of the composite. The different yarn angles in the interior, boundaries, and corners of the composite are also shown. Photographs of similar cross sections of a three-dimensional braided specimen are provided for comparison and verification of the constructed cross sections. It is also shown that the fiber architecture in the corners of the preform may vary depending on the number and arrangement of yarn carriers on the braiding machine. The different fiber architectures in the boundaries and corners are expected to affect the mechanical properties of the composite, and for the range of three-dimensional braided preforms currently produced, these effects may not be negligible.

Acknowledgment

The author would like to thank A. S. D. Wang of Drexel University under whose direction and supervision the braided preform described in this paper was fabricated.

References

- ¹Mohajerjasbi, S., "Structure and Mechanical Properties of 3-D Braided Composites," Ph.D. Thesis, Dept. of Mechanical Engineering, Drexel Univ., Philadelphia, PA, July 1993.
- ²Mohajerjasbi, S., "Modeling and Analysis of 4-Step 3-D Cartesian Braided Composites Including Axial Yarns," *Proceedings of the AIAA/ASME/ASCE/AHS/ASC 36th Structures, Structural Dynamics, and Materials Conference* (New Orleans, LA), AIAA, Washington, DC, 1995, pp. 8-16 (AIAA Paper 95-1157).
- ³Macander, A. B., Crane, R. M., and Camponeschi, E. T., Jr., "Fabrication and Mechanical Properties of Multidimensionally (X-D) Braided Composite Materials," *Composite Materials: Testing and Design* (Seventh Conference), edited by J. M. Whitney, ASTM STP 893, American Society for Testing and Materials, Philadelphia, PA, 1986, pp. 422-443.
- ⁴Gause, L. W., and Alper, J. M., "Structural Properties of Braided Graphite/Epoxy Composites," *Journal of Composites Technology & Research*, Vol. 9, No. 4, 1987, pp. 141-150.
- ⁵Mohajerjasbi, S., "Predictions for Coefficients of Thermal Expansion of 3-D Braided Composites," *Proceedings of the AIAA/ASME/ASCE/AHS/ASC 37th Structures, Structural Dynamics, and Materials Conference* (Salt Lake City, UT), AIAA, Reston, VA, 1996, pp. 1812-1817 (AIAA Paper 96-1531).

A. M. Waas
Associate Editor